Int. J. Electrochem. Sci., 12 **(2017)** 10933 – 10945, doi: 10.20964/2017.11.19

International Journal of
ELECTROCHEMICAL
SCIENCE
www.electrochemsci.org

A Highly Effective Copper Nanoparticle Coupled with RGO for Electrochemical Detection of Heavy Metal Ions

Dan Li[1], *Chongxu Wang*[2], *Hui Zhang*[2], *Youyi Sun*[2,*], *Qianqian Duan*[1], *Jianlong Ji*[1], *Wendong Zhang*[1], *Shengbo Sang*[1,*]

[1] Intelligent Control System of the Ministry of Education and Key Lab of Advanced Transducers & College of Information Engineering, Taiyuan University of Technology, Taiyuan 030024, China.
[2] Shanxi Province Key Laboratory of Functional Nanocomposites, North University of China, Taiyuan 030051, P.R.China.
[*]E-mail: sangshengbo@tyut.edu.cn

Received: 28 June 2017 / *Accepted:* 26 August 2017 / *Published:* 12 October 2017

A highly effective copper nanoparticle (CuNP) coupled with reduced graphene oxide was successfully prepared by liquid phase reduction. The as-prepared products were tested with X-ray diffraction, field-emission transmission electron microscopy, and scanning electron microscopy. CuNPs were distributed averagely on the surface of reduced graphene oxide. CuNP/RGO nanocomposites modified bare glassy carbon electrode was measured by electrochemical impedance spectroscopy and cyclic voltammetry. The availability of CuNP/RGO nanocomposites was analyzed by square wave anodic stripping voltammetry (SWASV). The nanocomposites showed a high electroanalytical activity and eximious sensitivity to Hg(II), Cu(II), Cd(II) and Pb(II), these ions exhibited sensitivities of 27.76, 25.86, 66.30 and 50.17 μA/μM, respectively, and the limits of detection were 0.051, 0.111, 0.203 and 0.186 μM, respectively. The CuNP/RGO nanocomposite was used firstly to detect individually and simultaneously various heavy metal ions. Furthermore, CuNP/RGO/GCE has good anti-interference properties and stability. In this study, CuNP/RGO nanocomposites are presented as a potential material to detect individually and simultaneously heavy metal ions.

Keywords: CuNP/RGO, SWASV, electrochemical measurement, heavy metals.

1. INTRODUCTION

Heavy metals are extremely harmful pollutants that affect biological system, because they are highly toxici, easy to accumulate, and difficult to be degraded. In addition, heavy metals are a serious threat to human health [1–3]. Hence, developing a high-speed, high sensitivity, and uncomplicated analysis method to detect and monitor heavy metal contaminants in water is considerably significant. Various techniques have been used for detecting trace heavy metals, including mass spectrometric [4],

optical [5], and electrochemical [6] methods. With the continuous progress of materials science, a clipping analytic, low power, highly sensitive, and flexible method for in-situ analysis must be developed [7]. Therefore, the method of electrochemical measurement for tracing heavy metals has drawn more attention.

The design and synthesis of electrode materials is a crucial step in the process of detecting heavy metal ions by electrochemical analysis method. Of all the electrode materials, metal nanoparticle-modified electrodes are known to markedly enhance electrochemical sensitivity because of numerous active sites, fast transfer speed and their large specific surface area [8, 9]. Now, varieties of nano-materials have been used to make electrochemical sensor, containing graphene, nanotubes, metal nanoparticles and some composite materials [10–13]. Of the various metal NPs, CuNPs exhibit the superior capacitance performance, which is mainly attributed to the considerably large surface area and enhanced electronic and ionic conductivities [14]. Thus, CuNPs are a desirable substrate in preparing chemically modified electrodes for electrochemical sensing. In addition, excellent sensitivity, small environmental hazards and low cost make RGO get more attention. Abundant carbonaceous materials, for instance CNTs [15, 16], graphene [17, 18], porous carbons [19, 20], carbon paste and carbon nanospheres [21], have been used to produce efficient electrochemical sensors in the past few years. Several sensitive sensors have been developed with graphene oxide and metal NP composites. Periyasami et al. fabricated AuNPs on RGO to detect and monitor toxic heavy metal ions and biocontrol bacterium as a scavenging agent [22]. Riyaz Ahmad Dar et al. constructed a composite material (sliverNP–graphene oxide) to detect As(III) [23]. Bin Zhang et al. fabricated AuNP/CNF hybrids for detecting heavy metal ions [24]. Qi wen Chen et al. prepared a graphene–CuNP nanocomposite via situ chemical reduction for electrochemical measuring of carbohydrates [25]. In addition, Wu et al. synthesized copper oxide nanowires with graphene for detecting pentachlorophenol [26]. However, the use of CuNP/RGO composites for detecting heavy metal ions, including Hg(II), Cu(II), Cd(II) and Pb(II), have been rarely studied. Thus, CuNP/RGO nanocomposites can be used as electrochemical sensor to detect heavy metals.

Given the aforementioned circumstance, liquid phase reduction was used in this study to synthesize CuNP/RGO nanocomposites. The glassy carbon electrode was modified by the CuNP/RGO nanocomposites and used as a novel electrochemical sensor to detect and quantify toxic substances in water, containing Hg(II), Cu(II), Cd(II) and Pb(II). The active surface area of electrochemical sensor was increased with CuNP/RGO modified elctrode, and the adsorption performance was also improved. In addition, the electrochemical sensor provides a quickly and highly sensitive current response, this result was ascribed to fast electron transfer between the solution and electrode. In this experiment, the cycling stability of working electrode and the mutual interference between heavy metal ions were carefully researched.

2. EXPERIMENTAL

2.1. Materials

In order to synthesis of CuNP/RGO nanocomposites, graphite was purchased from Shanghai Carbon Co, A.R.-grade H_2SO_4, $KMnO_4$, $NaH_2PO_2{\cdot}H_2O$, EDTA, DMF, ascorbic acid, $CuSO_4{\cdot}5H_2O$,

and H_2O_2 were obtained from Baiwan Chemical Reagent Co., Ltd (Shanxi, China). The aqueous solution containing heavy metal ions was obtained with the addition of solid $Hg(NO_3)_2$, $3CdSO_4{\cdot}8H_2O$, $Pb(NO_3)_2$, and $Cu(NO_3)_2$. To adjust the pH value, a certain amount of HNO_3 was added to the stock solution of heavy metal ion. The 0.1 M acetate buffer solution (HAc–NaAc, pH=5.0) was compounded with the addition of 0.1 M HAc and NaAc. The distilled water come from NANOpureDiamondTM UV system.

2.2. Apparatus

Surface morphology and nanometric structure of CuNP/RGO nanocomposites were recorded using a field-emission transmission electron microscope (TEM, JEOL 2100) and a field-emission scanning electron microscopy (FESEM, Hitachi S-4700). X-ray powder diffraction (XRD) patterns of CuNP/RGO nanocomposites was observed using a Rigaku Max-2200. Of all electrochemical measurements were completed on a ZAHNER-PP211 electrochemical workstation from Germany and a conventional three-electrode system. A bare glassy carbon electrode (GCE, 3 mm in diameter) was used as the working electrode, and the reference and counter electrodes were respectively Ag/AgCl (3.5 M KCl) and a platinium minigrid electrode.

2.3. Preparation of CuNP on the RGO sheets

The CuNP was obtained via liquid phase reduction. Firstly, GO was synthesized successfully from natural graphite via the Hummers method [39]. Generally, RGO can be prepared by using a strong reducing agent, such as $NaBH_4$, hydrazine hydrate. But they are a serious threat to human health and environment. Additionally, the oxygen containing functional groups on the GO surface were reduced by $NaBH_4$ and hydrazine hydrate, which leads to the decrease in sensor performance. To eliminate the adverse effect, a green and inexpensive synthetic method was used to reduce the GO. 0.02 g ascorbic acid was added to 50 mL GO dispersion (0.1 mg/mL) as a reducing agent. After the ultrasonic treatment, the mixture dispersion was placed for 48 h to obtain the RGO dispersion solution. An aqueous solution of $NaH_2PO_2{\cdot}H_2O$, EDTA (4 g/L), and $CuSO_4{\cdot}5H_2O$ (0.1 mol/L) were then mixed and heated with a water bath (70 °C); the molar ratio of $NaH_2PO_2{\cdot}H_2O$ to $CuSO_4{\cdot}5H_2O$ was 2.4, and the concentration ratio of EDTA (4 g/L) to $CuSO_4{\cdot}5H_2O$ (0.1 mol/L) was 1/4. When the reaction of mixed reactants was complete and the supernatant liquid was decanted, the precipitated powder was washed with distilled water, soaked with anhydrous ethanol to prevent oxidation, and then filtered and dried to obtain the CuNP powder. 1 mg of CuNP powder was then added to 40 mL DMF-dispersed RGO solution (2 mg/ml) via stirring for 2 h. The mixed solution was finally filtered and dried to obtain the CuNP/RGO nanocomposite. During the CuNP/RGO nanocomposite preparation, $NaH_2PO_2{\cdot}H_2O$ was added for direct reduction of the Cu ions on the RGO sheets.

2.4. Preparation of the CuNP/RGO/GCE

The bare glassy carbon electrode was polished using both 0.3 and 0.05 μm alumina slurries and flushed successively with absolute ethyl alcohol, HNO_3 (1:1), deionized water. Then, 20mg CuNP / RGO nanocomposite powder was scattered in 20mL ethanol. In order to form a uniform suspension, the 20 mL solvent mixture was treated with ultrasound for 3 hours. 4 μL solvent mixture was then added to the surface of glassy carbon electrode and made it dried at room temperature. The modified electrode, CuNP/RGO/GCE, was thus formed. For comparison, the RGO/GCE was fabricated using RGO solvent mixtures in accordance with the above method. To achieve the best reproducibility of the electrode preparation process, the GCE was polished for 30 min with both 0.3 and 0.05 μm alumina slurries. Ultrasonic frequency was 20 kHz, the ultrasonic time was 5 min, and the temperature was 20 ^{o}C. The modified GCE must be dried at room temperature, because high frequency and temperature lead to poor electrode performance, and the results of electrochemical measurements using cyclic voltammetry and EIS become inaccurate.

2.5. Electrochemical detection of Cd(II), Cu(II), Pb(II), and Hg(II)

Hg(II), Cu(II), Cd(II) and Pb(II) were detected individually and simultaneously, all of the detection and electrochemical analysis were performed with an ZAHNER-PP211 electrochemical workstation. The CuNP/RGO/GCE electrode was first placed in a solution mixed by heavy metal ions and buffer solution (HAc-NaAc). At a -1.5 V desorption potential vs. the SCE for 120 s, heavy metal ions were reduced from the mixed solution to the surface of electrode. And then added a reverse voltage on the working electrode for potential scanning, so that heavy metals re-oxidated into the ion into the mixed solution. The experimental parameters were set as follows: the frequency is 25 Hz, the period is 40 ms, the amplitude is 20 mV, the initial slope is 100 mV/s, the step potential is 5 mV, and the integral time is 2 ms. In addition, a positive potential of 60 s was applied to the modified electrode for removing residual heavy metal ions deposited on the electrode surface.

3. RESULTS AND DISCUSSION

3.1. CuNP/RGO nanocomposite's morphologic and surface properties

Fig. 1 shows the morphology and structure of CuNP/RGO nanocomposite, it revealed a crumpled and wrinkled RGO surface. Thus, the RGO provided the condition for CuNP attachment. Fig. 1b presents that CuNPs were attached to the surface of RGO sheets, demonstrating strong interaction among the CuNPs and RGO. TEM of the synthesized CuNP/RGO and RGO hybrids was presented in Fig. 1c-d, these also show the CuNPs attached to the surface of the RGO sheets. This phenomenon is attributed to the surface functional groups on the RGO sheets, which provide a large number of reactive sites for binding of CuNPs and nucleation. Hence, electrostatic bonding and charge transfer make CuNPs interact strongly on the RGO sheets.

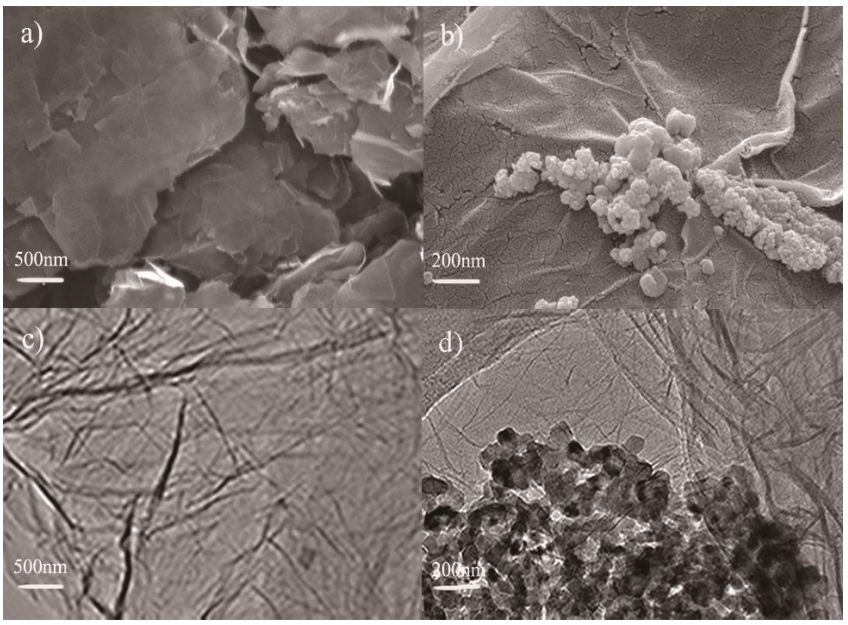

Figure 1. SEM images of RGO sheets and CuNP/RGO nanocomposite (a, b), TEM images of RGO sheets and CuNP/RGO nanocomposite (c, d).

Fig. 2 presents the XRD image of CuNP/RGO nanocomposite. The peaks at 43.3^o, 50.4^o, and 74.1^o were indexed to (111), (200), and (220) planes, respectively, of the Cu crystal. Besides, a obvious diffraction peak was observed at $2\theta = 23.6^o$, indicating the (002) planes of graphitic carbon in nanocomposite [24]. The result implies the presence of CuNPs on the RGO sheets, and this is consistent with the findings described above.

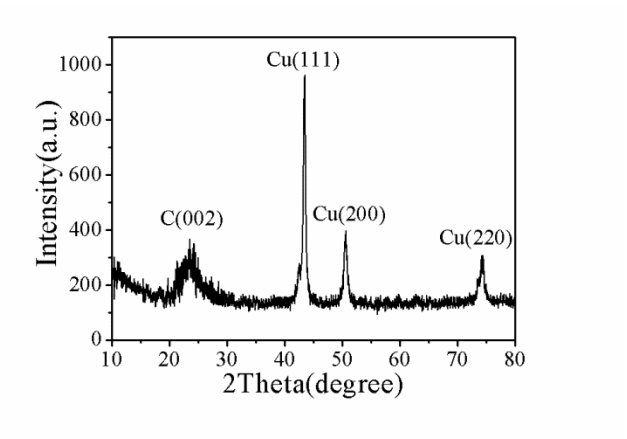

Figure 2. XRD pattern of CuNP/RGO.

3.2. Electrochemical characterization of the CuNP/RGO hybrids modified electrode

The cyclic voltammetry response of RGO and CuNP/RGO/GCE was measured in 2.5 mM $Fe(CN)_6^{-3/-4}$ solution (Fig. 3a). Compared with the peak current of GCE, the reduction and oxidation peak current of CuNP/RGO nanocomposite-modified GCE decreased. Meanwhile, the reduction and

oxidation peak current of CuNP/RGO nanocomposite-modified GCE were lower than those of RGO, indicating that the presence of CuNP/RGO nanocomposite delayed electron transfer. This effect could be attributed to multiple hydroxyl and epoxy groups of RGO sheets [27, 28], which could hinder ions diffusion and electrons transfer.

The electrochemical impedance spectroscopy of RGO and CuNP/RGO hybrids was also measured in 2.5 mM $Fe(CN)_6^{-3/-4}$ solution. As shown in Fig. 3b, the electron transfer resistance (Ret) is represented by a semi-circle in a high frequency range, and the linear segment characterises the diffusional limitation within a low frequency range[29]. The electron transfer resistance (Ret) of CuNP/RGO nanocomposite-modified GCE was about 108 Ω, and the double-layer capacitance was calculated to be about 66.5μF/cm (C = 1/2πmfz). The Ret value of GCE represents a considerably low electron transfer resistance. After modification with RGO, the CuNP/RGO nanocomposite, the Ret value further increased compared to GCE. This behavior suggests that the presence of CuNP/RGO nanocomposite can obstruct the electron transfer, these results are highly consistent with the aforementioned CV data.

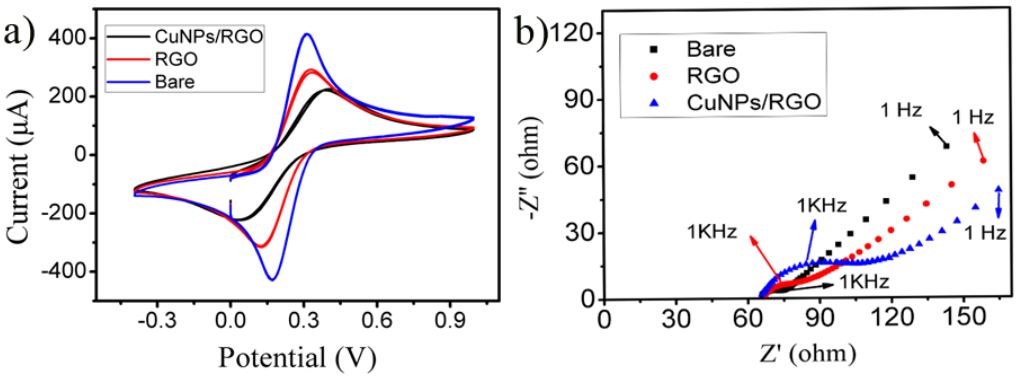

Figure 3. (a) Cyclic voltammetric responses and (b) electrochemical impedance spectra of RGO and CuNP/RGO modified GCE

3.3. Electrochemical determination of heavy metal ions with the CuNP/RGO/GCE

Under the similar experimental environment, Hg(II), Cu(II), Cd(II) and Pb(II) were detected individually and simultaneously using CuNP/RGO nanocomposite-modified GCE. Fig. 4a shows SWASV responses to Pb(II) in the concentration range of 0.05–3.0 μM in 0.1 MHAc–NaAc (pH=5.0) under a deposition potential of −1.0 V for 150 s. Obviously, the peak of Pb(II) was clearly observed at -0.57 V. The regression equation was i/μA =82.63 + 50.15c/μM, and the correlation coefficient was 0.983. The value of Pb(II) electrochemical sensing was 50.15μA/μM. The limit of detection (LOD) was 1.86×10^{-7} M (using the 3σ method). The sensitivity and LOD in this study and previously detected values for heavy metals electrochemical sensing with other modified electrodes are summarized in Table 1. These results show that high sensitivity with respect to heavy metals was obtained using CuNP/RGO nanocomposite-modified electrode. This phenomenon was ascribed to the larger electrochemically active surface area, the high surface free energy and effective acceleration of the electron transfer among the electrode and solution,which resulted in a high current response. Under the

same experimental conditions, Fig. 4b shows the response to Cd(II) about linear relationship between the peak currents and the concentrations from 0.05 μM to 2.0 μM by the SWASV method; the peak was observed at −0.77 V. The linearization equation was i/μA = 3.56 + 66.3c/μM, the sensitivity was 66.3 μA/μM, the LOD was 2.03×10^{-7} M. In addition, the electrochemical response to Hg(II) and Cu(II) at concentrations ranging from 0.05 μM to 2.5 μM and from 0.5 μM to 1.0 μM, respectively, are shown in Fig. 4c-4d, respectively. The two peaks were clearly observed at 0.28 V and −0.03 V. The regression equation of Hg(II) and Cu(II) were i/μA =14.88 + 27.76c/μM (R^2=0.976) and i/μA = 9.92+25.86c/μM (R^2=0.986). The sensitivity of Hg(II) and Cu(II) were 27.76 and 25.86 μA/μM, the LODs were 5.1×10^{-8} and 1.11×10^{-7} M.

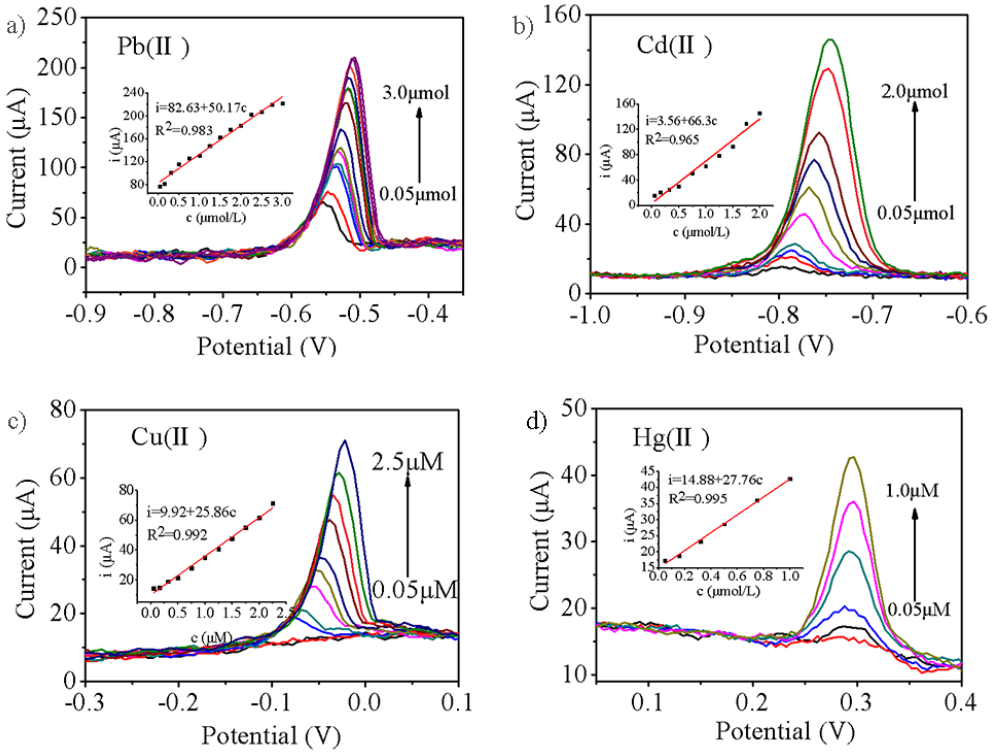

Figure 4. (a–d) SWASV responses and the corresponding calibration plots of CuNPs/RGO modified GCE for individual detection towards Pb(II), Cd(II), Cu(II), and Hg(II) at different concentrations in 0.1 M HAc–NaAc buffer solution (pH=5.0).

Simultaneous detection of Hg(II), Cu(II), Cd(II) and Pb(II) was then conducted at different concentrations under a deposition potential of -1.0 V for 150 seconds. The corresponding results are presented in Fig. 5a. When different heavy metal ions produced the reduction reaction on the CuNPs/RGO-modified electrode, different constant potentials were required for polarization, and this resulted in peaks of heavy metal separation. The separated stripping peaks for Hg(II), Cu(II), Cd(II) and Pb(II) were obviously observed at +0.32, -0.05, -0.74 and -0.56 V, as shown in Fig. 5b. The individual detection results were nearly the same. Therefore, Cd(II), Pb(II), Hg(II) and Cu(II) could be simultaneously detected with the CuNP/RGO/GCE.

Table 1. Comparison of current sensitivity and LOD obtained using different electrodes for heavy metals detection .

Electrodes	Heavy metals	Sensitivity (μA/μM)	LOD(μM)	Ref.
CuNPs/GO/GCE	Pb(II)	50.17	0.186	This work
	Cd(II)	66.3	0.203	
	Cu(II)	25.86	0.111	
	Hg(II)	27.76	0.051	
AuNPs/RGO/GCE	Pb(II)	47.76	12.69 nM	22
	Cd(II)	19.05	31.81 nM	
	Cu(II)	22.10	27.42 nM	
	Hg(II)	29.28	20.70 nM	
BandFe3O4/RGO/GCE	Pb(II)	13.6	0.169	30
	Cd(II)	4.35	0.04	
	Cu(II)	10.1	0.05	
Fe3O4/MWCNTs/GCE	Pb(II)	11.4	6.0 pM	31
MnO2/GCE	Pb(II)	22.4	---	32
	Cd(II)	18.05	---	
rGO/MWCNTs GCE	Pb(II)	42.1	0.052	33
SnO2/graphene/GCE	Pb(II)	18.6	0.0018	34
	Cd(II)	18.4	0.1015	
	Cu(II)	5.16	0.1141	
	Hg(II)	2.766	0.0344	
Porous Co3O4/GCE	Pb(II)	71.5	0.018	35

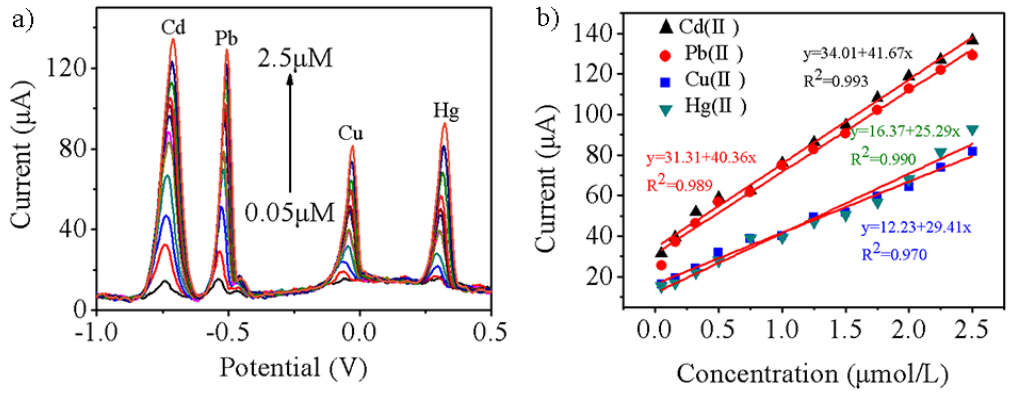

Figure 5. (a) SWASV responses and (b) the corresponding calibration plots for the simultaneous detection of Hg(II), Cu(II), Pb(II) and Cd(II) in the concentration range of 0.05–2.5 μM on the CuNPs/RGO nanocomposite-modified GCE in 0.1 M HAc–NaAc buffer solution (pH=5.0).

Table 2 presents the correlation coefficients, sensitivities and LODs individually and simultaneously detected different heavy metal ions. When Cd(II), Pb(II), Hg(II) and Cu(II) were detected simultaneously, the sensitivity of Cu(II) was significantly enhanced, it could be ascribed to the presence of a Hg film in process of enrichment [36]. Meanwhile, sensitivities with respect to

Hg(II), Cd(II) and Pb(II) were significantly decreased, it could be ascribed to the sorption of ions in mixed solution [37]. The hanging mercury drop electrode [38] is extensively used in the electrochemical measurement.

Table 2. Comparison of individual and simultaneous analyses towards Cd(II), Pb(II), Hg(II) and Cu(II).

	Analyte	LOD(μM)	Correlation coefficient	Sensitivity(μA/μmol)
Individual analysis	Pb(II)	0.186	0.983	50.17
	Cd(II)	0.203	0.965	66.3
	Cu(II)	0.111	0.992	25.86
	Hg(II)	0.051	0.995	27.76
Simultaneous analysis	Pb(II)	0.131	0.989	40.36
	Cd(II)	0.103	0.993	41.67
	Cu(II)	0.225	0.970	29.41
	Hg(II)	0.130	0.990	25.29

3.4. Interesting mutual interferences

To analyze the phenomenon of mutual interferences when Hg(II), Cu(II), Cd(II) and Pb(II) exist simultaneously, we evaluated the effects of concentrations of Pb(II) or Cd(II) on the oxidation peak currents of other heavy metal ions. Figure 6a shows the electrochemical response of CuNP/RGO nanocomposite-modified electrode in a concentration range of 0.05–2.0 μM with respect to Pb(II) in the existence of each 1.0 μM Hg(II), Cu(II) and Cd(II) ions 0.1 M buffered solution (NaAc–HAc). The concentrations of Pb(II) interfered with the oxidation peak currents of the other three heavy metal ions is presented in Fig. 6b, as the concentration of Pb(II) increased, the peak current increased linearly, the sensitivity of Pb(II) was 24.47 μA/μM. The figure also illustrates a continuous decrease in the peak currents of 1.0 μM Cd(II) as the concentration of Pb(II) added. The peak current of Cu(II) ascended obviously, whereas the peak current of Hg(II) slightly decreased. The peak current of Hg(II) and Cu(II) gradually became stable with the concentration of Pb(II) increased. The behavior was attributed to the existence of a Pb film and Hg–Pb and Pb–Cu intermetallic compounds in the deposition process [34], and these can improve the sensitivity for Cu(II). When Pb(II) had a low concentration, a sufficient number of Pb(II) ions were needed to form the film. Thus, when Pb(II) concentration was relatively high, the stripping peak was significantly enhanced.

Fig. 6c reveals the electrochemical response of CuNP/RGO nanocomposite-modified electrode in a concentration range of 0.05–2.5 μM with respect to Cd(II) in the existence of each 1.0 μM Hg(II), Pb(II) and Cu(II) in buffered solution (NaAc–HAc). The figure also shows how the concentrations of Cd(II) interfered with the anodic peak currents of the three other heavy metal ions. Meanwhile, Fig. 6d indicates that a favorable linear relationship of Cd(II) was obtained with a sensitivity of 20.07 μA/μM. In addition, the peak current of 1.0 μM Pb(II) increased initially and then decreased when the concentration of Cd(II) exceeded 0.5 μM. The peak currents of Hg (II) and Cu (II) increased at the

same time, but the peak current of Hg (II) increased obviously. As the concentration of Cd(II) increased, the peak currents of Cu(II) and Pb(II) gradually became stable. This result could be ascribed to the existence of a Cd film and Hg–Cd and Cd–Cu intermetallic compounds [34], and these increase the sensitivity of Cu(II). With a continuous increase in the concentration of Cd(II), the peak current of Hg(II) and Cu(II) became to be stable, which could be ascribed to the formation of Cd film on the surface of working electrode.

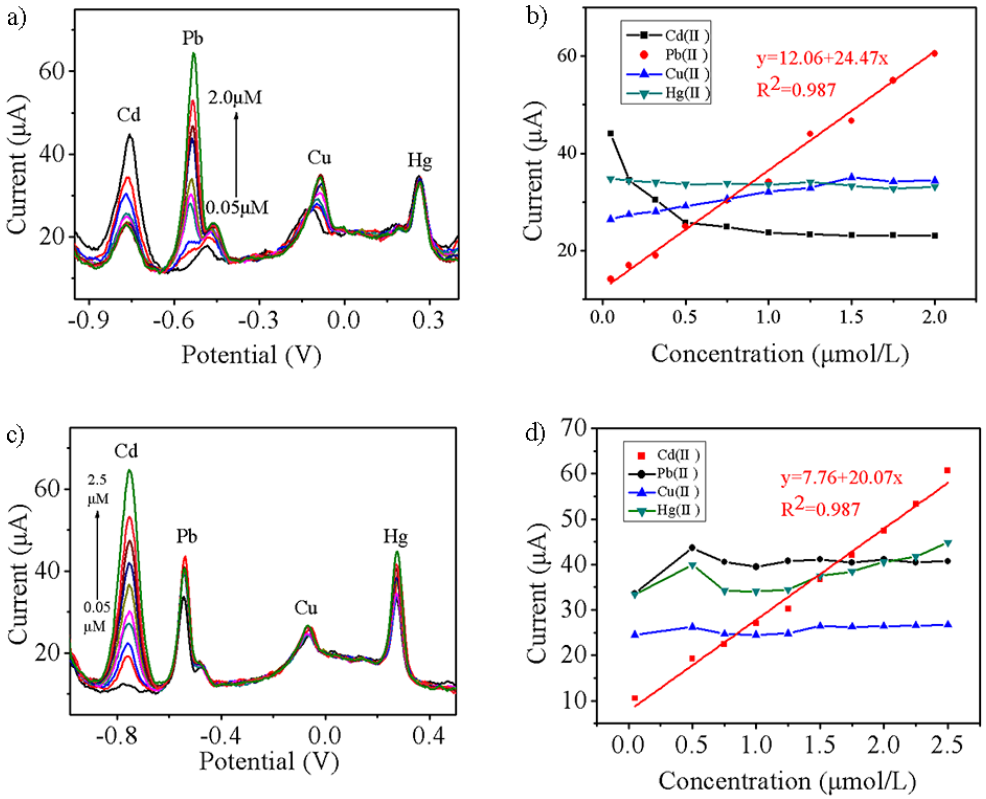

Figure 6. SWASV responses and corresponding calibration plots of the CuNP/RGO nanocomposite-modified electrode: (a) and (b) for Pb(II) in the concentration range of 0.05–2.0 μM in the presence of each 1.0 μM Cd(II), Cu(II), and Hg(II) ions in 0.1M NaAc–HAc solution (pH=5.0); (c) and (d) for Cd(II) in the concentration range of 0.05–2.5 μM in the presence of each 1.0 μM Pb(II), Cu(II), and Hg(II) ions in 0.1 M NaAc–HAc solution (pH=5.0).

3.5 Stability measurement

The reproducibility of CuNP coupled with reduced graphene oxide nanocomposite-modified electrode is vital for electrochemical detection in various areas of application. In addition, recyclability and reversibility are also rather critical. Fig. 7a reveals the reproducibility of electrode modified with CuNP/RGO nanocomposite, Hg(II) at a concentration of 1.0 μM was detected in buffer solution (HAc–NaAc) after 9 cycling tests at different times within 7 day. The stripping currents were nearly constant after 9 cycling tests. The result implys CuNP/RGO nanocomposite-modified electrode has excellent recyclability. The peak current was 98.36% of the original peak current after 9 cycling tests

at different times within 7 day. These results indicate the electrode modified with CuNP/RGO nanocomposite exhibited good reversibility and cycling stability.

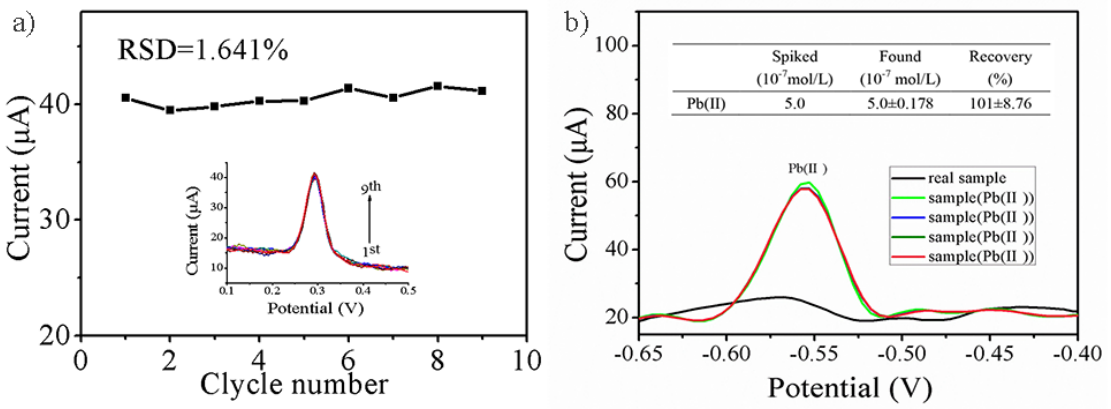

Figure 7. (a) SWASV responses to Hg(II) from the 1st to the 9th cycle and (b) SWASV responses for four standard additions of Pb(II) in the diluted water sample. The inset table is the recovery calculation.

Table 3. Recovery of individual analyses towards Cd(II), Hg(II) and Cu(II).

	Spiked (10^{-7}mol/L)	Found (10^{-7} mol/L)	Recovery (%)
Cd(II)	6.0	6.0 ± 0.134	100 ± 7.64
Cu(II)	7.0	7.0 ± 0.193	101 ± 9.25
Hg(II)	8.0	8.0 ± 0.117	100 ± 5.82

3.6. Application to real water analysis

In order to analyze the practicability of CuNP/RGO nanocomposite-modified electrode, 100 mL water was collected from Jinyang lake in Taiyuan City, Shanxi, China, and the suspension material was quickly filtrated. Pb(II) was choosen as a typical ion. The pH of water sample was adjusted to 5.6 with 0.1 M HAc–NaAc, and no evident peak for Pb(II) was detected (the black line in Fig. 7b). This implied that the content of Pb(II) was lower than 0.05 μM/L. 0.5 μM/L Pb(II) solution was then added to the diluted water sample, and this was measured in parallel 4 times using SWASV. The results are shown in Fig 7b, an obvious peak for Pb(II) was observed at −0.56V, the recovery was calculated to be 101% ± 8.76%. Additionally, Cd(II), Hg(II) and Cu(II) in water samples were examined by the same method and recoveries were shown in Table 3. This result indicates CuNP/RGO nanocomposite-modified electrode has potential value in practical applications.

4. CONCLUSIONS

In this study, A highly effective copper nanoparticle (CuNP) coupled with reduced graphene oxide was successfully prepared via a facile method. The high-performance electrode modified by CuNP/RGO nanocomposite was used as the working electrode to determinate heavy metal ions individually and simultaneously, such as Hg(II), Cu(II), Cd(II) and Pb(II). The electrochemical results indicate that CuNP/RGO nanocomposite-modified electrode exhibited a high sensitivity for individual and simultaneous detection of Hg(II), Cu(II), Cd(II) and Pb(II). In addition, a mutual interference was implemented between the four heavy metal ions' detection and the change in concentrations of Cd(II) and Pb(II). Between the stripping peaks, the potential separation was sufficiently large. This study demonstrated the presence of Cd(II) or Pb(II) can improve sensitivity with respect to Hg(II) and Cu(II). This occurrence was attributed to the presence of a Cd film or Pb film. Although interference occurred between the four ions, it did not affect the simultaneous detection. Finally, the excellent stability of the CuNP/RGO nanocomposite renders the material potentially useful in the field of electrochemical determination.

ACKNOWLEDGEMENTS
This work was supported by the Doctoral Fund of MOE of China (No.20131402110013), 863 project (2015AA042601) and the National Natural Science Foundation of China (No.51505324, 61501316, 61474079, 61471255, 51622507).

References

1. F. B. Edward, C. K. Yap, A. Ismail, and S.G. Tan, *Water. Air. Soil. Poll*, 196 (2009) 297.
2. R. Khlifi, and A. Hamza-Chaffai, *Toxicol. Appl. Pharm*, 248 (2010) 71.
3. S. K. Yadav, *S. Afr. J. Bot*, 76 (2010) 167.
4. I. Ugulu, *Appl. Spectrosc. Rev*, 50 (2015) 113.
5. L. N. Neupane, E. T. Oh, H. J. Park, and K. H. Lee, *Anal. Chem*, 88 (2016) 3333.
6. S. M. Choi, D. M. Kim, O. S. Jung, and Y. B. Shim, *Anal. Chim. Acta*, 892 (2015) 77.
7. M. B. Gumpu, S. Sethuraman, and U. M. Krishnan, *Sensor. Actuat. B-chem*, 213 (2015) 515.
8. C. Marichy, M. Bechelany, and N. Pinna, *Adv. Mater*, 24 (2012) 1017.
9. L. Matlock-Colangelo, and A. J. Baeumner, *Lab. Chip*, 12 (2012) 2612.
10. H. Im, X. J. Huang, B. Gu, and Y. K. Choi, *Nat. Nanotechnol*, 2 (2007) 430.
11. J. Lu, I. Do, L. T. Drzal, R. M. Worden, and I. Lee, *Acs. Nano*, 2 (2008) 1825.
12. N. J. Ronkainen, H. B. Halsall, and W. R. Heineman, *Chem. Soc. Rev*, 39 (2010) 1747.
13. J. Wang, *Chem. Rev*, 108 (2008) 814.
14. A. Ehsani, B. Jaleh, and M. Nasrollahzadeh, *J. Power. Sources*, 257 (2014) 300.
15. Y. Shao, J. Wang, H. Wu, J. Liu, I. A. Aksay, and Y. Lin, *Electroanal*, 22 (2010) 1027.
16. J. Li, S. Guo, Y. Zhai, and E. Wang, *Electrochem. Commun*, 11 (2009) 1085.
17. M. M. Radhi, W. T. Tan, M. Z. Ab Rahman, and A. B. Kassim, *Res. J. Appl. Sci*, 5 (2010) 59.
18. Y. Liu, Y. Li, and X. Yan, *Adv. Funct. Mater*, 18 (2008) 1536.
19. X. Nie, and W. Hu, *Anal. Scl*, 26 (2010) 141.
20. A. Stein, Z. Wang, and M. A. Fierke, *Adv. Mater*, 21 (2009) 265.
21. L. Zhang, W. Li, Z. Cui, and W. Song, *J. Phys. Chem*. C, 113 (2009) 20594.
22. P. Gnanaprakasam, S. E. Jeena, and D. Premnath, *Electroanal*, 28 (2016) 1885.

23. R. A. Dar, N. G. Khare, and D. P. Cole, S. P. Karna, *Rsc. Adv*, 4 (2014) 14432.
24. B. Zhang, J. Chen, H. Zhu, T.Yang, M. Zou, and M. Zhang, *Electrochim. Acta*, 196 (2016) 422.
25. Q. Chen, L. Zhang, and G. Chen, *Anal. Chem*, 84 (2011) 171.
26. W. Wu, H. Xiao, S. Luo, C. Liu, Y. Tang, and L. Yang, *Sensor. Actuat. B-chem*, 222 (2016) 747.
27. H. He, J. Klinowski, M. Forster, and A. Lerf, *Chem. Phys. Lett*, 287 (1998) 53.
28. A. Lerf, H. He, M. Forster, and J. Klinowski, *J. Phys. Chem*. B, 102 (1998) 4477.
29. Y. Wei, L. Kong, R. Yang, L. Wang, and J. Liu, *Chem. Commun*, 47 (2011) 5340.
30. Y. Sun, W. Zhang, H. Yu, C. Hou, D. Li, and Y. Zhang, *J. Alloy. Compd*, 638 (2015) 182.
31. Y. Yang, Y. You, Y. Liu, and Z. Yang, *Microchim. Acta*, 180 (2013) 379.
32. Q. Zhang, H. Wen, D. Peng, Q. Fu, and X. Huang, *J. Electroanal. Chem*, 739 (2015) 89.
33. J. Zhang, Z. Jin, W. Li, W. Dong, and A. Lu, *J. Mater. Chem*. A, 1 (2013) 13139.
34. Y. Wei, C. Gao, F. Meng, H. Li, and L. Wang, *J. Phys. Chem*. C, 116 (2011) 1034.
35. Z. Liu, X. Chen, J. Liu, and X. Huang, *Electrochem. Commun*, 30 (2013) 59.
36. C. Gao, X. Yu, R. Xu, and J. Liu, *Acs.Appl. Mater. Inter*, 4 (2012) 4672.
37. Y. Sun, W. Chen, W. Li, T. Jiang, and J. Liu, *J. Electroanal. Chem*, 714 (2014) 97.
38. M. A. Ferreira, and A. A. Barros, *Anal. Chim. Acta*, 459 (2002) 151.
39. Y. Zhang, H. Chi, W. Zhang, Y. Sun, Q. Liang, and Y. Gu, *Nano-Micro. Lett*, 6 (2014) 80.